Energy Reports 10 (2023) 3197–3210

Contents lists available at ScienceDirect

Energy Reports

journal homepage: www.elsevier.com/locate/egyr

Research Paper

Impact of building integrated photovoltaics on high rise office building in the Mediterranean

Alba Ramos [a], Joaquim Romaní [b,*], Jaume Salom [b]

[a] Department of Graphic and Design Engineering, Barcelona School of Industrial Engineering, Universitat Politècnica de Catalunya, Avda. Diagonal 647, 08028 Barcelona, Spain

[b] Catalonia Institute for Energy Research (IREC), Thermal Energy and Building Performance Group, Jardins de les Dones de Negre, 1, 08930 Sant Adrià De Besòs, Barcelona, Spain

ARTICLE INFO

Keywords:
Solar energy
Building simulation
Transparent BIPV
Renewable energy
Photovoltaic
PV glazing

ABSTRACT

Building integrated photovoltaics (BIPV) presents a great opportunity for decreasing building energy demand and related CO_2 emissions, specially in the refurbishment of old isolated high rise highly glazed office buildings. This article presents a simulation study of the impact of BIPV on a Spanish office building of the 60's, aiming to serve as a reference for this type of buildings in the Mediterranean region. Upgrade of the envelope with BIPV is evaluated. The solutions for the glazing system include conventional solar control window and a transparent photovoltaic prototype window. On the opaque part, commercial BIPV is considered. A comprehensive model integrating the BIPV impact in walls in windows for the thermal, electrical and daylighting is presented. Dynamic simulations carried out with TRNSYS software allow to evaluate the impact on daylighting, energy demand and economics. The results show that transparent BIPV reduced the energy demand by 6.9% and the total energy balance by 21%. The opaque BIPV further improved these results achieving a 38.3% reduction in the energy balance. Moreover, transparent BIPV also reduces the hours with excessive daylighting, although at the cost of reduced daylighting autonomy. The economic analysis highlights the importance of electricity pricing schedules in the promotion of BIPV, comparing current tariff structure in Spain and the duck chart from California Independent Operator. Results show the capabilities of this technology and provides guidelines for investment cost and efficiency targets.

1. Introduction

Buildings energy consumption currently represents about 40% of the global energy consumption, and it is forecasted to continue growing in the coming decade (IEA, 2019, 2020). At the same time, energy-related CO_2 emissions from buildings have risen in recent years, challenging the goal of reducing greenhouse gases (GHG) emissions to meet a 1.5 °C world or below (IPCC, 2018). The continued use of fossil fuel-based energy sources, a lack of effective energy-efficiency policies, and insufficient investment in sustainable buildings is translated into an untapped important emissions reduction potential.

The improvement of buildings energy efficiency and on-site renewable energy generation are key factors to achieve the goals of the sustainable development scenarios (SDS) by 2030. In this regard, the EU's directives introduced the concept of net zero-energy buildings (NZEB) (The European Commission, 2010, 2012). Which is complemented by Europe aims to be the first climate-neutral continent by 2050 (The European Commission, 2019). The application of the NZEB model in Europe became mandatory at the end of 2020 for all new buildings. However, the latest directive updates extended the NZEB challenge to all existing buildings in long-term renovation strategies (Magrini et al., 2020; The European Commission, 2018).

In this context, solar energy, and in particular Building Integrated Photovoltaics (BIPV), presents the best opportunities for energy generation adapted to buildings design (Biyik et al., 2017). BIPV systems allow on-site renewable electricity generation integrating photovoltaics (PV) by replacing conventional building components or materials, i.e. in facades, roofs, windows or skylights. BIPV solutions will also impact on the thermal and lighting loads, as well as the electricity output and occupant comfort of the building.

Despite both opaque and transparent (or semi-transparent) BIPV solutions can be found, of particular interest are the latter. Opaque BIPV systems typically consider crystalline silicon cells; as it is the most

* Corresponding author.
E-mail address: jromani@irec.cat (J. Romaní).

https://doi.org/10.1016/j.egyr.2023.09.178
Received 10 February 2023; Received in revised form 28 August 2023; Accepted 28 September 2023
Available online 7 October 2023

Nomenclature

Abbreviations

BIPV	Building integrated photovoltaics
BSDF	Bidirectional scattering distribution function
CFS	Complex fenestration system
DA	Daylight autonomy
EB	Energy balance
PV	Photovoltaics
PV_{op}	Opaque BIPV
PV_{tr}	Transparent BIPV
RF	Reference
SC	Solar control
SHGC	Solar heat gain coefficient
U-value	Thermal transmittance
WWR	Window-to-wall ratio
β_T	PV efficiency thermal coefficient
η_{ref}	PV nominal efficiency

Subindex

fa	Façade
fl	Floor
lim	Limit
nren	Non-renewable
prim	Primary energy
tot	Total
wi	Window

strongly established technology on the market and presents relatively low prices (Fraunhofer, 2020; Kumar et al., 2017; IRENA, 2020). However, in the last years, thin film PV cells and other emerging low-cost PV technologies have been rapidly identified as interesting for BIPV systems (Fraunhofer, 2020). These technologies present a semi-transparency in the visible range, allowing a wide new range of building integration possibilities (Biyik et al., 2017; Quesada et al., 2012; Jelle et al., 2012). Moreover, most of these semi-transparent PV technologies small thickness makes them flexible while having aesthetics very close to those of standard buildings fenestration systems (Attoye et al., 2017; Ramanujam et al., 2020).

The number of publications on BIPV solutions has significantly increased in the recent years. Despite the vast majority of the publications used to be limited to modelling and energy performance calculations of opaque BIPV solutions, the number of articles studying semi-transparent BIPV solutions is rapidly increasing. Among the semi-transparent BIPV studies found, a large percentage of them consider glazing systems with inhomogeneous transparency, where the percentage of light that passes through is due to a separation space between encapsulated opaque PV cells (cell cladding) (Sánchez-Palencia et al., 2019; Meraj and Khan, 2019; Pranith and Bhatti, 2015; Bambara and Athienitis, 2019; Roeleveld et al., 2015; Xiong et al., 2022). In (Sánchez-Palencia et al., 2019; Meraj and Khan, 2019; Pranith and Bhatti, 2015) modelling and analytical expressions for solar cells performance of cell cladding BIPV are presented. Design of greenhouses considering cell cladding BIPV is addressed in (Bambara and Athienitis, 2019). In (Roeleveld et al., 2015) the validation of a CFD model of a cell cladding type BIPV system is presented, and in (Xiong et al., 2022) the effect of time-changing shadows on cell cladding BIPV performance is studied.

Fewer studies address the simulation and/or testing of BIPV solutions considering thin-film or emerging PV technologies, but these studies rarely consider the building energy performance. In example, in (Virtuani and Strepparava, 2017) a model is proposed to describe the daily performance ratio of amorphous (a-Si) and crystalline silicon (c-Si) BIPV solutions under real operating conditions, and in (Bellazzi et al., 2018) a module of ceramic tile with integrated a silicon amorphous thin film solar cell was tested in working conditions. In (Alrashidi et al., 2022) thermal performance of Cadmium telluride (CdTe) based semi-transparent PV glazing of different transparencies in the UK was evaluated. Results revealed that the use of least transparency PV glazing can reduce 96% of solar heat gains and 23.2% of cooling energy compared to conventional clear glazing when used in South-West orientation. In (Meng et al., 2018), again the energy performance of semi-transparent CdTe thin film PV window on commercial buildings in Hong Kong is evaluated. Results show large energy saving potential in Hong Kong, between 15% and 20%, compared to a-Si PV window and a common window.

Other studies assess building energy performance considering BIPV or BIPV/T solutions. In (Saadon et al., 2016), a numerical simulation of a partially transparent (cell cladding), ventilated PV façade of an office building is presented. In (Goncalves et al., 2020) authors develop a multi-physics BIPV model for the simulation of BIPV facades for building and district energy simulations. In (Yang et al., 2020) results of numerical simulation for the performance prediction of BIPV/T double-skin façade are presented. Different BIPV materials were considered in this study as the façade cladding of an office building located in Australia, concluding that integrating the Perovskite-based solar cell solution the highest energy savings were achieved. In (Freitas et al., 2020) a feasibility study is conducted using Rhinoceros CAD software and plugins Grasshopper and Ladybug to assess BIPV envelopes for office buildings in Brazil. In (Chen et al., 2021) authors developed a new parametrization scheme for BIPV windows and incorporated it into building energy simulations coupled with a single-layer urban canopy model. In (Azami and Sevinç, 2021) a methodology for a parametric study to determine the optimal building envelope to meet international Passive House standard (PHS) standard is presented. In (Sun et al., 2021) a comprehensive mapping tool is proposed to investigate the feasibility of BIPV applications, by introducing a quantitative visual impact assessment in addition to the traditional energy yield projections. The main conclusion from these studies is that BIPV systems provide significant potential for reducing building energy needs, in addition to the electricity production from the PV cells. Moreover, the importance of the integration of BIPV (both opaque and transparent) and building behaviour to model the thermal, electrical, and daylighting calculation is stated. None of the aforementioned studies present an economic assessment of the BIPV solutions studied. This work aims to fill these gaps presenting a comprehensive model for BIPV simulation, considering real BIPV optical data, and addressing an economic evaluation of the proposed solutions.

The refurbishment of old office buildings with BIPV in the Mediterranean region is a topic scarcely tackled in the literature. The case study for this research is the GESA building, Fig. 1, an emblematic office building in Palma de Mallorca (Spain). Despite of its iconic and protected status, the GESA building has been abandoned for several years, hence it requires a refurbishment that will also update its skin to the current energy efficiency standards. The case study is an example of the office buildings representative of the architectural trends of the 60 s, following the international line of Modern architecture, some examples are shown in Fig. 2.

This work addresses a simulation study of the impact of BIPV taking as reference a representative floor of the aforementioned GESA building. Section 2 presents the methodology with the modelling approach and the adapted model for transparent PV. Section 3 describes the case of study, with the building current characteristics and the new glazing systems and BIPV solutions. Section 4 presents the energy, daylighting,

Fig. 1. Current state of the GESA building, picture by authors.

and economic results, which are further discussed in Section 5, with the conclusions being summarised in Section 6.

The novelty of this work relies on: i) the comprehensive building model integrating the BIPV impact in walls in windows for the thermal, electrical and daylighting simulation based on a modification of TRNSYS18 complex fenestration model (Romaní et al., 2021a, 2021b), ii) the energy performance assessment of a novel homogeneous semi-transparent BIPV solution (developed under the framework of the Tech4win project (Tech4win, 2019)) which performance is compared with alternative solutions for a real building and the economic assessment of the proposed solution studied, iii) the evaluation of the electricity pricing schedule into the feasibility of BIPV. Finally, results obtained from this work are not only applicable to the analysed building but to other high rise highly glazed buildings; thus, aiming to serve as a reference for this type of buildings in the Mediterranean region.

2. Methodology

The simulations are carried out with TRNSYS18 (TESS, 2017), a graphically based software environment used to simulate the behaviour of transient systems. The building is modelled with 'Type 56', a component designed to model detailed multi-zone building (TRANSSOLAR, 2018). The 3D model is developed with Sketchup and uploaded to TRNSYS with a specific plugin. The modelling assumptions and the case study are defined in Section 3.

2.1. Transparent BIPV modelling (PV_{tr})

The TRNSYS detailed multi-zone building component does not include a specific model for transparent BIPV (PV_{tr}) integrated in windows. Hence, a modified version of the complex fenestration system (CFS) model developed is used. The CFS implemented in TRNSYS allows the calculation of the optical and thermal behaviour of a window composed of up to six layers including external and internal shading systems (Hiller and Schöttl, 2014). This model uses the ISO 15099 (2003) (ISO 15099, 2003) energy balance and bidirectional scattering distribution function (BSDF) for optical calculations. The modified version introduces the PV generation in the energy balance of the window panes, see Fig. 3.

The BSDF allows to calculate the total reflected radiation of the window, the total transmittance, as well as the absorption in each window pane. Then Eq. (1) calculates the absorbed and transmitted radiation in the pane where the PV cell. Finally, the PV cell efficiency and output are calculated with Eq. (2). Previous research presents the model details and the relevant parameters (Romaní et al., 2021a). The model has already been used to study the impact of a prototype transparent PV glazing (Romaní et al., 2021b).

$$G_{\tau\alpha.i} = G_t - G_r - \sum_1^{i-1} \dot{S}_n \tag{1}$$

$$\dot{P}_{PV.i} = \eta_{ref}\left[1 + \beta_T\left(T_i - T_{ref}\right)\right] G_{\tau\alpha} \tag{2}$$

Where $\dot{P}_{PV.i}$ PV output at "i" window pane [W·m^{-2}]; η_{ref} PV cell nominal efficiency [-]; β_T: Temperature coefficient [%·K^{-1}]; T_i temperature of the window pane [ºC]; T_{ref} reference temperature of PV cell nominal efficiency calculation, 25 ºC; $G_{\tau\alpha}$ transmitted and absorbed solar radiation at the window pane "i" [W·m^{-2}]; G_t global solar radiation incident to the window [W·m^{-2}]; G_t reflected solar radiation [W·m^{-2}]; and $\dot{S}_n$ absorbed solar radiation at the previous window pane "n" [W·m^{-2}].

2.2. Opaque BIPV modelling (PV_{op})

The opaque BIPV (PV_{op}) is model with 'Type 567–5' (TESS, 2013), which is designed to interact with the multi-zone building 'Type 56'. It assumes that the PV panels operate under maximum power point

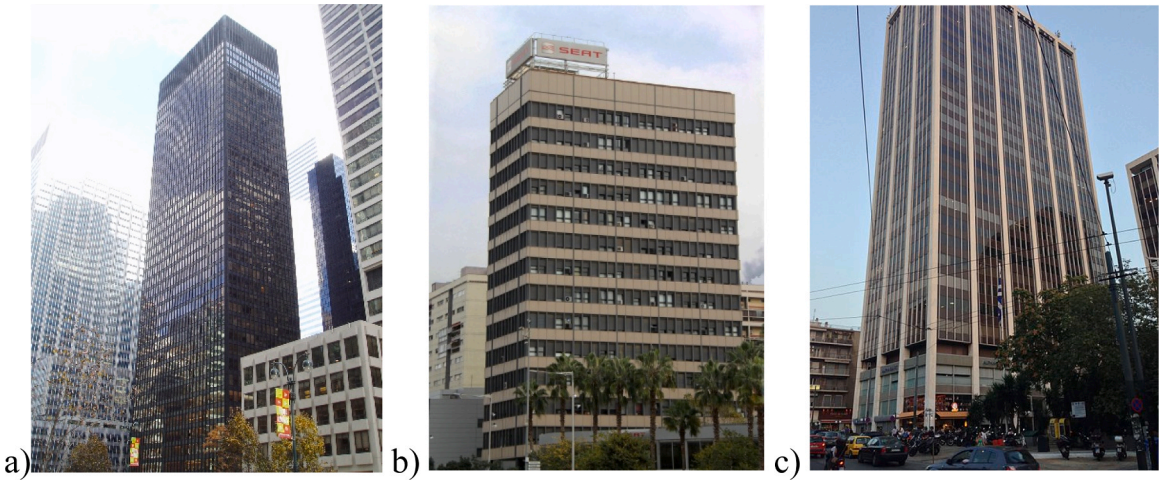

Fig. 2. Some images of Modern architecture buildings of the 60 s a) Seagram building in New York (Seagram Building, 2022), picture by Steve Cadman licensed under CC BY-SA 2.0, b) SEAT building in Barcelona (Edifici Seat, 2022), picture by Albert Esteves and published with the permission of the author and c) Athens Tower in Athens (Athens Towers, 2022), picture by Dimitris Kamaras licensed under CC BY-SA 2.0.

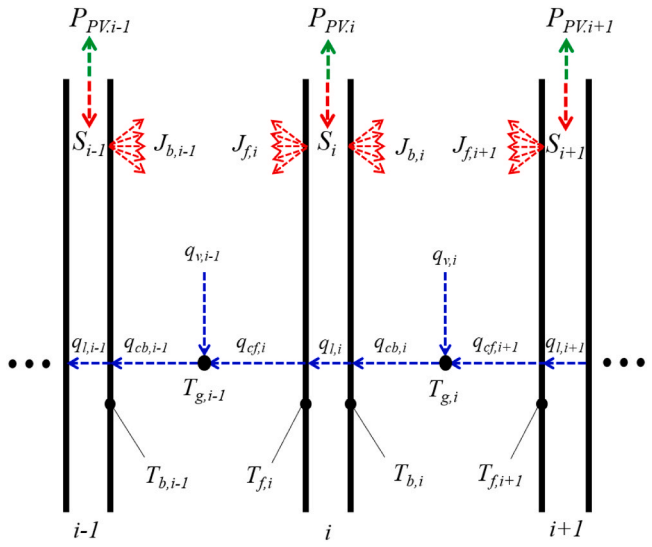

Fig. 3. Modified ISO 15099 window energy balance including the PV output (Romaní et al., 2021a).

conditions, with the efficiency being calculated with linear modifying factors dependent of the temperature and radiation (equivalent to Eq. (2)). The absorbed radiation is calculated with the angle of incidence and refractive index of the cover. The 'Type 576–5' are connected to the 'Type 56' assuming no flow in the channel, hence assuming the convection heat transfer coefficients of an air-gap.

2.3. Daylighting

The daylight conditions of the zones are calculated with the DaySIM approach inbuilt to TRNSYS 'Type 56' (TRANSSOLAR, 2018). This evaluates the illuminance conditions in sensor points inside the zones. Note that the daylighting scripts in built into 'Type 56'' do not interact with the CFS. As the current research does not use complex or movable shades, hence no significant discrepancy in the daylight results is expected.

2.4. Evaluation indicators

2.4.1. Energy

The façade and window properties will affect the heating, cooling, and lighting loads of the building. Additionally, in case of considering a BIPV solution, there will be electricity generation. The energy performance of the building is calculated using the final energy for heating, cooling, dehumidification, ventilation, lighting and PV generation. The equipment consumption is also taken into account, so that the total electrical load of the building can be calculated together in terms of PV self-consumption potential. Consequently, the solutions are evaluated with the final energy balance (Olivieri et al., 2014) described in Eq. (3). Note that the only energy carrier considered is electricity.

$$E_{\{balance\}} = E_{\{heating\}} + E_{\{cooling\}} + E_{\{lighting\}} + E_{\{ventilation\}} + E_{\{equipment\}} - E_{\{photovoltaics\}} \quad (3)$$

2.4.2. Daylighting

The selected parameters to evaluate the daylight performance are the daylight autonomy (DA), and the hours with excessive illuminance. The DA measures the fraction of occupancy hours in which the daylight illuminance in the reference point is above the minimum required illuminance, as in Eq. (4). The minimum illuminance is set to 500 lux, according to recommended illuminance values from EN 12464-1 (European Committee for Standardization, 2011) for working spaces in office buildings.

Illuminance above 2000 lux is considered to cause too bright environments which might lead to visual discomfort as well as glare risk (Nabil and Mardaljevic, 2005; Reinhart et al., 2006). The excessive illumination is calculated as the fraction of occupancy hours with illuminance above the threshold, Eq. (5).

$$DA = \frac{\sum_{t=0}^{t=8760}\left(t_{(Ill_t>500)}\cdot occ_t\right)}{\sum_{t=0}^{t=8760}(occ_t)} \quad (4)$$

$$Ex.ill = \frac{\sum_{t=0}^{t=8760}\left(t_{(Ill_t>2000)}\cdot occ_t\right)}{\sum_{t=0}^{t=8760}(occ_t)} \quad (5)$$

Where DA is the daylight autonomy [-], Ex.ill is the excessive illuminance [-]; t is the time step [h]; Ill_t is the illuminance at the time step [lux]; occ_t indicates if there is occupancy at the time step [-].

2.4.3. Economic

The economic impact is evaluated with the discounted payback period, which calculates the number of years required to achieve a positive net present value (NPV). The NPV accounts for the investment cost of the retrofit solution and the cash flow (CF) considering a discount rate to account for the time-value of money (d), see Eq. (6). As a retrofit solution, the CF is the difference between the reference system operational expenditures (OPEX) and the OPEX minus the incomes of the new solution, see Eq. (7).

$$NPV = \sum_{j=0}^{N}\frac{CF_i}{(1-d)^j} - CAPEX_i \quad (6)$$

$$CF_i = OPEX_{ref.i} - (OPEX_i - Incomes_i) \quad (7)$$

The CAPEX accounts only for the components and installation cost of the new windows, the opaque PV, and the inverters. These are summarised in Section 3.4.3.

In the study the OPEX accounts only for the cost of electricity, assuming that the façade maintenance will be similar with all solutions and that the replacement period is longer than the payback. The schedule of the electricity tariff is key to the viability of PV solutions. The "current" scenario represents the present Spanish electricity schedule. Spain has an intermediate penetration of renewables, with up to 38% in 2019 (International Energy Agency, 2021). The "current" electricity schedule for workweek days in Spain follows the demand, with price "peak" in the morning and late afternoon, a "flat" (intermediate) price in the afternoon, and a "valley" period in the night. However, the energy transition is expected to change the electricity pricing schemes. The "high PV" scenario mimics the California Independent Operator the duck chart, in which net load resulting of high penetration of photovoltaics presents a very low price, called "super-valley", in the mid-day hours (Denholm et al., 2015). The "current" and "high PV" electricity schedules are taken from the Syn.ikia project (SYNIKIA, 2021), as shown in Fig. 4. The average electricity price is 0.23 €/kWh as taken from Eurostat for Spain (Eurostat, 2021). The average electricity price is used to calculate the "current" schedule "peak", "flat", and "valley" tariffs. Then, the "high PV" chart scenario uses the same range of prices with the "super valley" tariff being calculated proportionally. Note that independently of the scenario, during weekends the electricity

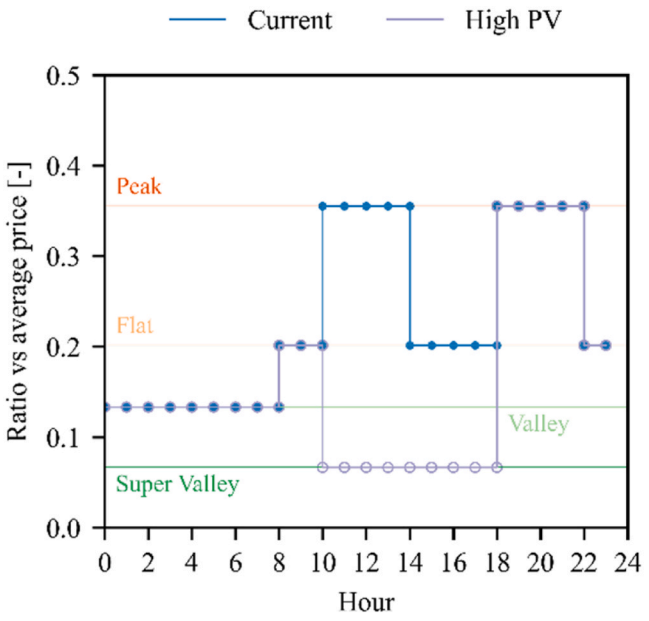

Fig. 4. Electricity price schedules (SYNIKIA, 2021).

price is constant at the "valley" price.

The case of study does not consider batteries; hence any overproduction of the PV will be injected to the grid. Therefore, the compensation scenario for the exported electricity is relevant to the economic evaluation. Three compensation scenarios are considered: feed-in tariffs of 0% (no compensation), 30% (typical value in Spain), and 100% (net-metering) of the current electricity price. In any case, the monthly bill cannot be negative (incomes higher than expenses).

Finally, the discounted payback is calculated assuming a discount rate of 5% and an average electricity price increase of 1.2%. The latter is obtained from Spain average harmonised indices of consumer prices (HCIPs or inflation rate) from 2010 to 2019 (Eurostat, 2022).

3. Case of study

The case study is a representative floor of the GESA building in Palma de Mallorca (Spain) (Paricio, 2015), a high rise building constructed in the 60 s testimony of the Modern Movement in Mallorca. It is characterized by its glazed curtain wall Fig. 1. Despite the iconic status, the GESA building has been empty for almost a decade, with the degradation issues related to abandonment. Nevertheless, the GESA building is protected by the local heritage commission, which is interested in its refurbishment and recommissioning to avoid further damage. The inefficient envelope, location (isolated and in a sunny climate), and representability of a typology of office building makes it a good reference for studying the impact of refurbishing with BIPV. Yet, the local heritage commissioning demands to keep the aesthetics and design on the envelope, in order to keep the GESA building recognisable image. Hence, implementation of BIPV in both the opaque and transparent sections of the façade is limited by the aesthetics and geometry of the existing construction system. Finally, note that because of the abandonment state of the building no data is available to calibrate the simulation models. Consequently, the results will be verified against similar studies on highly glazed office buildings (Pascual et al., 2010) and the Spanish building code (Código técnico de la edificación, 2019).

3.1. Building model characteristics

The 3D model of this multi-floor building is simplified modelling a single representative floor with its corresponding boundary conditions (reference floor). As shown in Fig. 5 above, the reference floor presents

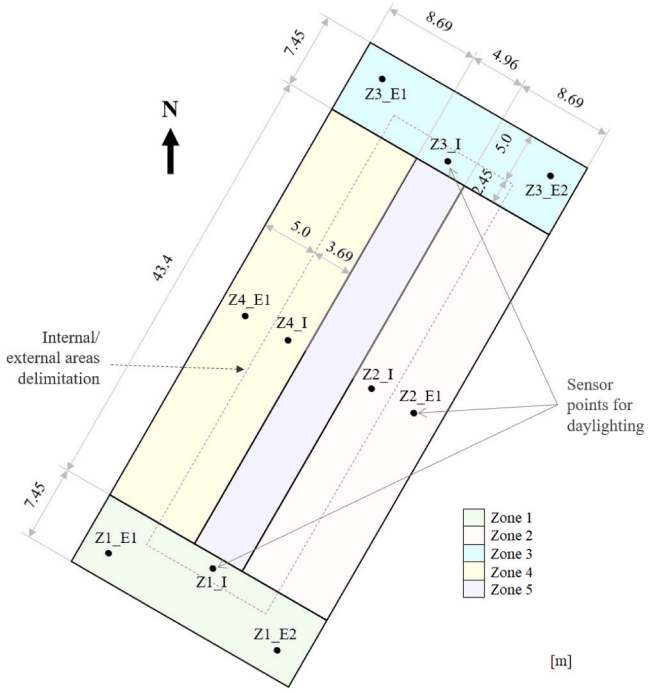

Fig. 5. Top view of a representative floor of the GESA building and its orientation, together with daylight sensors positioning.

an inner rectangular area where elevators, stairs and other services are located, surrounded by an open space limited by the building façade (curtain wall).

When developing the 3D model the reference floor is divided into 5 different zones, the open space represented by zones South, East, North, and West and the service are by the central zone. The 3D model of the reference floor developed is shown in Fig. 6. The walls between zone 5 and the rest of the zones are defined as partition walls, while the walls between the zones composing the open space are defined as fictitious internal windows, with 100% transparency and solar heat gain coefficient (SHGC) and low thermal resistance representing the convection heat exchange. The actual building will have a mass flow exchange between the zone depending on the temperature and pressure variations. However, modelling this effect is beyond the scope of the study, for which the energy balance of the windows and BIPV solutions is calculated. Another simplification is merging all the windows in a same façade, Fig. 6, while ensuring that the window and frame surface are the same than in the actual building.

In Tables 1–3, the reference floor and zones, the façade wall and the inner walls characteristics are summarised. Note that the façades walls defined in Table 2, for the reference case, and Table 3, for the opaque BIPV façade, correspond to the yellow area in Fig. 6. Finally, the inner wall characteristics are defined in Table 4. The ceiling and floor surfaces of the reference floor are defined as 'boundary', meaning that the heat transfer through these surfaces is zero. This simulates the effect of having above and below another floor of identical characteristics. The detailed characteristics of the windows modelled are presented in subsection 3.4 below.

The Spanish building code energy saving document (Código técnico de la edificación, 2019) requires that the sectors up to 5 m from the external façades have an independent daylighting control. Consequently, the East and West zones are divided in two sectors and the South and North zone in three, as shown in Fig. 5. The daylight sensors in the outermost sectors are placed a 2.5 m of the façade, while the ones in the inner sectors are placed at the sector centre. All the daylight sensors are placed at 0.85 m over the surface and control the lighting of the whole surface of their sector.

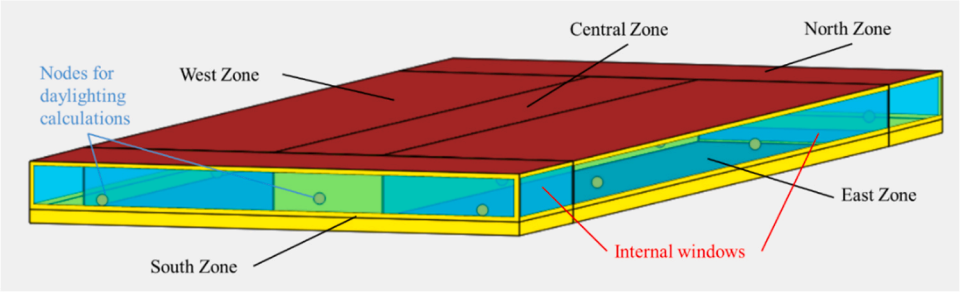

Fig. 6. 3D model of the reference floor of the GESA building.

Table 1
Reference floor and zones characteristics.

Zone	Parameter	Value
South	Volume [m^3]	443.88
	Floor area [m^2]	166.25
	Façade area [m^2]	21.96
	Window area [m^2]	77.43
	Window to wall ratio (WWR) [%]	77.4
	Capacitance [kJ/k]	9529.1
East	Volume [m^3]	1006.40
	Floor area [m^2]	376.93
	Façade area [m^2]	25.61
	Window area [m^2]	90.27
	Window to wall ratio (WWR) [%]	77.8
	Capacitance [kJ/k]	21,605.3
North	Volume [m^3]	443.88
	Floor area [m^2]	166.25
	Façade area [m^2]	21.96
	Window area [m^2]	77.43
	Window to wall ratio (WWR) [%]	77.4
	Capacitance [kJ/k]	9529.1
West	Volume [m^3]	1006.40
	Floor area [m^2]	376.93
	Façade area [m^2]	25.61
	Window area [m^2]	90.27
	Window to wall ratio (WWR) [%]	77.8
	Capacitance [kJ/k]	21,605.3
Central	Volume [m^3]	575
	Floor area [m^2]	215
	Façade area [m^2]	-
	Window area [m^2]	-
	Window to wall ratio (WWR) [%]	-
	Capacitance [kJ/k]	12,338.8

Table 2
Original façade wall characteristics.

Façade wall (curtain wall) composition and properties		Value
Composition	Particle wood [m]	0.010
	Common brick [m]	0.120
	Air gap	-
	Polystyrene [m]	0.015
	Maroon tempered glass [m]	0.010
Total thickness [m]		0.155
U-value [W/m^2K]		0.926

Table 3
BIPV façade wall characteristics.

Façade wall (curtain wall) with BIPV composition and properties		Value
Composition	Particle wood [m]	0.010
	Common brick [m]	0.120
	Air gap	-
	Polystyrene [m]	0.015
	BIPV opaque module [m]	0.014
Total thickness [m]		0.159
U-value [W/m^2K]		0.852

3.2. Operation regimes

The performance of the case study is modelled for a full year, with a simulation time step of 0.1 h (6 min). The case study assumes the weekly occupancy schedule of a generic office building, as presented in Fig. 7. The internal gains are considered proportional to the occupancy schedule, with the nominal values of sensible, latent, specific electrical power, and radiative fraction nominal values presented in Table 5.

The lighting gains also depend on the continuous lighting control. The illumination at these nodes will be evaluated by the software leaving the lighting ON when there is occupancy and the illuminance set point (500 lux) is not reached, and dimming the lighting to the required power otherwise. The lighting consumption and heat gains is calculated independently per each daylight sector, according to the sensors and subdivisions presented in Fig. 5.

The air renovation rate for ventilation is 2 ACH, according to the Spanish ventilation requirements (IDAE, 2012), and 0.32 ACH for infiltration, based on authors experience in old office buildings. Heating operates with a set-point of 21 ºC and a set-back of 18 ºC during non-occupancy hours. Cooling operates with a set-point of 26 ºC during occupancy hours and 30 ºC the rest of the hours. A dehumidification control is also implemented. Humidity set-point is 50% during occupancy hours from January to May and from October to December, 60% during occupancy hours from June to September and 100% the rest of the time. All these parameters values follow the indications of the Spanish building code (Código técnico de la edificación, 2019). Heating, cooling and dehumidification needs are covered by an electrically-fed reversible heat pump with a COP of 3.5 and an EER of 2.2. Ventilation electricity consumption is calculated assuming a linear correlation of 2.5 kW per m^3/s.

3.3. Climatic zone

The GESA building is located in Palma de Mallorca (Spain). The main characteristics of this climate are presented in Table 6. The simulations are carried with a typical meteorological year (TMY) weather file produced with Meteonorm.

3.4. Modelling scenarios

The façade of the reference building is a curtain wall composed by semi-transparent window area (~ 77%) and opaque area (~ 23%). The study considers five different scenarios: a reference scenario (RF) and

Table 4
Inner wall characteristics.

Inner walls composition and properties		Value
Partition wall composition	Gypsium plasterboard [m]	0.013
	Common brick [m]	0.120
	Gypsium plasterboard [m]	0.013
Total thickness [m]		0.146
U-value [W/m^2K]		2.004

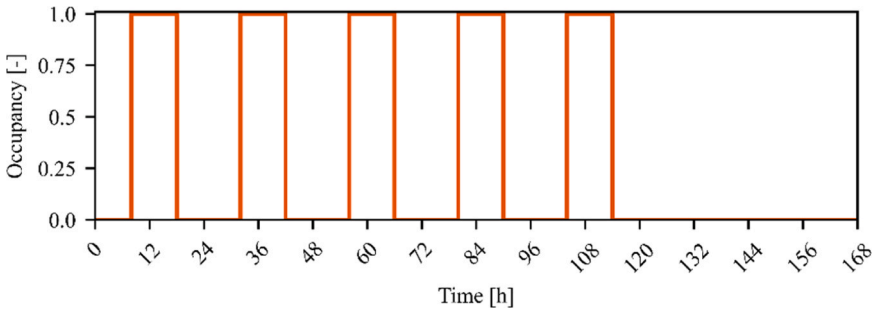

Fig. 7. Weekly occupancy schedule.

four more considering two different window solutions (a solar control window and semi-transparent BIPV) and two different façade solutions (the same as in the reference case and an opaque BIPV solution). The reference scenario (RF) scenario reproduces the current building envelope, with the façade characteristics presented in Table 3 (subsection 3.1) and the existing double glazing Parsol Bronze window. The solar control scenario (SC) upgrades the reference case by replacing the windows with the Solar Control glazing. The third case (SC+PV_{op}) improves the façade wall with opaque BIPV and the window with Solar Control glazing. The fourth and fifth case use transparent BIPV for the windows, one with the existing façade in the opaque part (PV_{tr}) and the other with opaque BIPV in the walls (PV_{tr}+PV_{op}).

The characteristics of the different windows as well as the characteristics of the opaque BIPV modelled are presented below. The façade wall characteristics when no opaque BIPV is considered are presented in subsection 3.1.

3.4.1. Windows

The reference window in this study is a double glazing Parsol Bronze window with an air-chamber. Two other window solutions will be also studied: a Solar Control and a transparent BIPV window (PV_{tr}). The Solar Control and BIPV windows use the same double glass structure but with a reflective coating on the back side of the front glass and considering a PV_{tr} glass as front glass, respectively. The Parsol Bronze and the Solar Control windows are modelled using the glass data from the International Glazing Data Base (IGDB) (Lawrence Berkeley National Laboratory, 2021). The spectral properties of the BIPV window are obtained from preliminary results of a transparent building solution from Tech4win project (Tech4win, 2019). This prototype of transparent BIPV window consist of tandem structure with and organic PV (OPV) cells and UV multifunctional cell. On one side, the OPV cell provides most of the electricity output. On the other, the UV multifunctional cell filters the UV radiation that might damage the OPV, while also generating electricity output. Laboratory measurements provided the refraction indices of each layer of the stack. These were processed with Filmwizard software to obtain the spectral properties of the stack. The thermal conductivity of each layer was obtained from literature sources. The data is processed with OPTICS6 (Lawrence Berkeley National Laboratory, 2013) to generate the glass file that will be used in WINDOW7 (Lawrence Berkeley National Laboratory, 2022) to generate the whole glazing system.

In Fig. 8 the transmittance properties of the modelled windows together with those of a clear glass are presented. It can be seen that the Parsol bronze window already have some solar control properties, with lower transmittance than a clear window in the infra-red, although losing a lot of visible transmittance. The selected solar control window has excellent selective behaviour, with a centred peak of visible transmittance but nearly null transmittance in the infra-red. The prototype PV_{tr} window has a similar transmittance peak in the visible range, with high absorption in the near infra-red due to its PV absorbed. Its transmittance in the infra-red is also lower than the Parsol bronze, although worse than the solar control window.

The configuration of the modelled windows and relevant centre of glazing properties calculate with WINDOW7 (Lawrence Berkeley National Laboratory, 2022) are summarised in Table 7. As expected from the optical properties described before, the Parsol Bronze has the highest SHGC and visible transmittance (T_{vis}), together with a high thermal transmittance due to its poor insulation. The solar control window presents the best thermal performance, with very low U-vale and SHGC. Due to the lack of coating, the BIPV window has a poor U-value,

Table 5
Sensible heat gains per type, radiative fraction and specific power.

Gain Type	Sensible heat gain [W/m^2_{fl}]	Radiative fraction [-]	Latent gain [W/m^2_{fl}]	Specific power [W/m^2_{fl}]
People	7.32	0.5	5.5	-
Equipment	7.81	0.7	-	7.81
Lighting	5.56	0.2	-	

Table 6
GESA building climate zone characteristics.

Reference city	Palma de Mallorca
Yearly average temperature [°C]	18.2
Annual solar incident radiation on horizontal surface [kWh/m^2]	1700
Yearly average relative humidity [%]	71

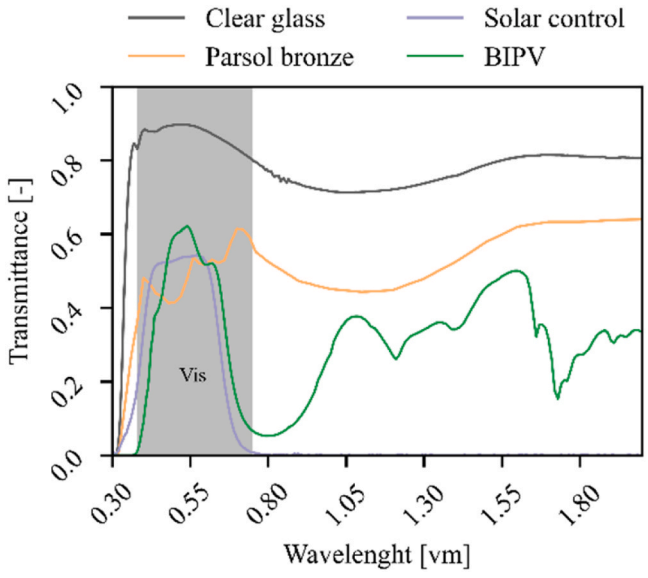

Fig. 8. Modelled windows glass transmittance, data obtained from IGDB (Lawrence Berkeley National Laboratory, 2021).

Table 7
Configuration, thermal transmittance (U), solar heat gain coefficient (SHGC) and visible transmittance of the modelled windows.

Window	Glazing system	U [W/m$^2_{wi}$K]	SHGC [-]	T_{vis} [-]
Parsol Bronze	SGG Parsol bronze 6 mm air 12.7 mm Planiclear 6 mm	2.787	0.577	0.439
Solar Control	SGG Diamant 50–22 6 mm Argon 16 mm Planiclear 6 mm	1.121	0.246	0.323
BIPV	PV_{tr} prototype. Air 12 mm SGG Planitherm XN 6 mm	1.601	0.326	0.319

although the SHGC improves compared to the Parsol Bonze. Yet, the visible transmittance is the worst.

Finally, the BIPV window (PVTR) is modelled with a nominal efficiency of (η_{ref}) 5.0% and a temperature coefficient of (β_T) of − 0.25%/K. These data correspond to the most up to date efficiency obtained testing laboratory scale devices in the framework of the European project Tech4win (Tech4win, 2019).

3.4.2. Opaque BIPV

As mentioned above, the opaque area of the building façade is proposed to be refurbished with an opaque BIPV (PV_{op}) solution. These replace the maroon tempered glass, see Table 2, with a BIPV panels of similar aesthetics from a commercial BIPV solution (Solar Module, 2022). The PV_{op} efficiency (η_{ref}) is 16.9% and its temperature coefficient (β_T) − 0.34%/K. The PV_{op} is modelled using Type 567–5 of BIPV model coupled to type 56.

3.4.3. Investment cost

The component and installation cost of the components is obtained from BEDEC construction materials database (BEDEC, 2022), except for the PV_{tr} window as it is a prototype. In this case the PV_{tr} window cost is considered assuming that the PV glass cost 200 €/m$^2_{wi}$ more than a clear glass, and the cost is extrapolated to a double-glazing window, as summarised in Table 8. The building has 271.52 m$^2_{wi}$ of windows and 95.14 m$^2_{fa}$ of opaque façade. In this study the PV_{tr} and PV_{op} are implemented in all four façades, with the estimated peak power for each BIPV scenario and the corresponding number of inverters is summarised in Table 9.

4. Results

4.1. Energy

4.1.1. Final energy use

The final energy consumption of the studied cases is presented in Fig. 9 and Table 10. The improved SHGC of the solar control and transparent PV windows, in comparison to the reference (RF), help to decrease the cooling demand between 27% and 31% in the PV_{tr}+PV_{op} and SC cases, respectively. Regarding the heating demand, the solar control window helps to slightly decrease it by virtue of its better thermal transmittance. However, the transparent PV causes an increase in the heating load since the high SHGC reduces the solar gains that would offset the heating demand. Moreover, the PV generation

Table 8
Investment and installation cost.

Component	Component cost	Installation cost
Solar control window	85.26 €/m$^2_{wi}$	17.675 €/m$^2_{wi}$
PV_{tr}	228.29 €/m$^2_{wi}$	17.675 €/m$^2_{wi}$
PV_{op}	141.37 €/m$^2_{fa}$	17.675 €/m$^2_{fa}$
Inverter 1500 VA	459.83 €/u	100.17 €/u

Table 9
Peak power and required number of inverters.

Case	Peak power [kW]	Number of inverters
PV_{op}	6.1	5
PV_{tr}	5.3	4
PV_{tr}+PV_{op}	11.5	8

effectively reduces the SHGC, as part of the absorbed radiation is converted to electricity instead of heat. Noticeably, the opaque PV helps to reduce the heating load while barely affecting the cooling demand. On the lighting side, the solar control and transparent PV have lower visible transmittance, hence the artificial lighting demand increases, as the rooms are below the illuminance set-point more often. As a result, the best improvement in energy demand is found for the solar control window with opaque PV (SC+PV_{op}) although the best final energy balance ($E_{balance}$) is achieved combining transparent and opaque PV (PV_{tr}+PV_{op}), as it has higher PV generation. Note that around 31% of the PV generated is exported to the grid, mainly because there is no demand during the weekends that can absorb this consumption, but also since the peak generation in intermediate seasons is often higher than the electricity demand.

4.1.2. Verification of energy results

The GESA building has been abandoned for several years and there is no operation data to calibrate the simulation model. As the focus of the study is to compare the impact of different BIPV solutions, the significance of the energy performance is compared against previous studies on highly glazed office buildings and the Spanish regulations.

On the one hand, obtained results are compared with the TOBEE project (Pascual, 2015), in which energy performance of different façades solutions and operation modes office buildings in Barcelona are evaluated. The TOBEE project uses a sample reference room of 9 m depth, and 3 m height, very similar to the GESA building, although with only a 5 m façade. As TOBEE assumes that the reference room is in contact with equivalent rooms, the consumption per square metre is comparable to GESA building. The specific TOBEE case taken as reference is window solution façade in a lighting optimisation scenario. In Table 11, the heating and cooling electricity demand of the case study are compared to the results of the TOBEE project. In order to make a fair comparison, the case of study building electricity demand has been adjusted to the efficiency values considered in the TOBEE project: heating COP of 1.58 and cooling EER of 2.02. The heating and cooling demands are within the TOBEE project ranges. The heating to be close to the maximum value and the cooling to be in the lower band, may be explained due to the different internal loads assumptions and building shape together with different operation regimes (i.e. set-points) and climatic conditions.

On the other hand, the Spanish building code (Código técnico de la edificación, 2019) sets a limit on annual non-renewable primary energy use per square metre and annual total primary energy use depending on the climatic zone and the internal gains. According the Spanish reference values for conventional electricity in the Balearic Islands, the primary energy factors for electricity are 2.968 and 3.049 kWh_{prim}/kWh_{fin} (IDAE, 2016). In Table 12, the building performance parameters according to the Spanish building code are compared with those obtained for the reference scenario (RF) in this study. The primary energy of the case of study considered is consistent with the regulated limits. Note that the simulations consider a highly efficient lighting and a reversible heat pump in all cases, including the reference scenario (RF). The later makes the reference scenario to be within the primary energy limits and very close to the non-renewable limit. The Spanish building code also requires complying with a solar protection criterion, measured as the solar gains during July ($q_{sol,jul}$). Here the reference case is above the limit, as expected by the poor performance of the Parsol Bronze windows and the absence of any solar protection.

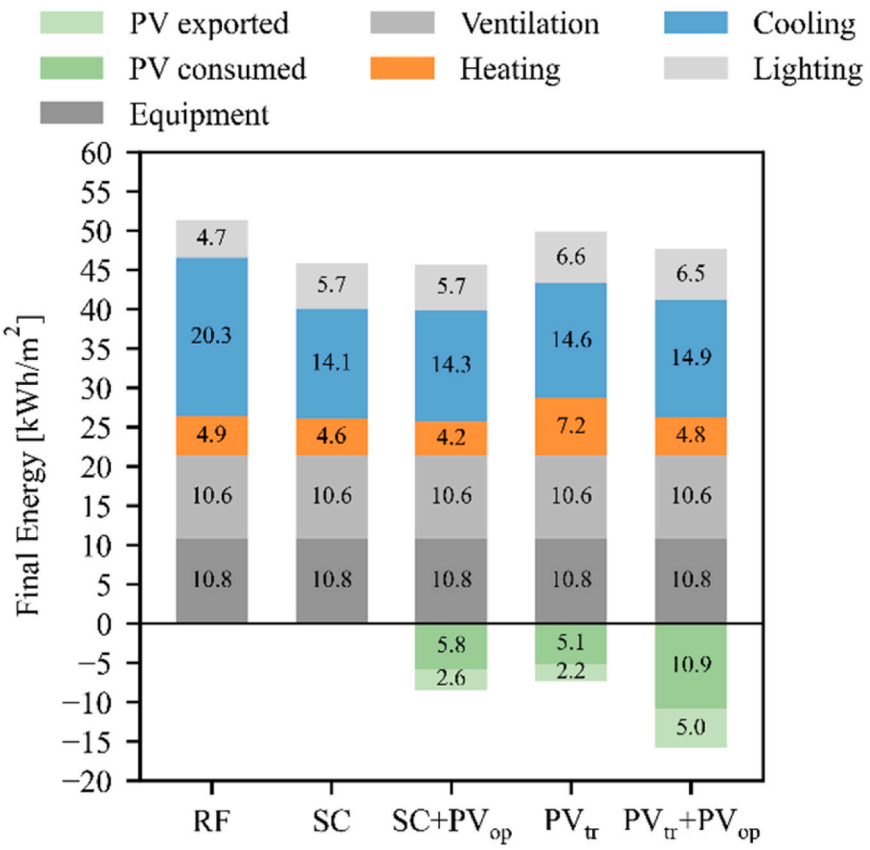

Fig. 9. Final energy consumption.

Table 10
Final energy change.

Final energy change (compared to RF)				
	SC	SC +PV_{op}	PV_{tr}	PV_{tr} +PV_{op}
Heat	-6.1%	-13.7%	47.8%	-1.5%
Cool	-30.6%	-29.6%	-27.8%	-26.3%
Light	22.3%	22.0%	41.0%	39.8%
Vent	0.0%	0.0%	0.0%	0.0%
Tot	-10.6%	-11.0%	-2.7%	-6.9%
$E_{balance}$	-10.6%	-27.6%	-17.1%	-37.9%

Table 11
Electricity demand of the case study compared to the results of TOBEE project for window solution façade in a lighting optimisation scenario (Pascual, 2015).

Parameter	TOBEE		GESA
	Min	Max	RF
Heat [kWh/m^2/year]	2.2	12.1	10.9
Cool [kWh/m^2/year]	14.4	50.0	22.1

Table 12
Building performance parameters according Spanish building code. Total primary energy ($E_{prim.tot}$), total non-renewable primary energy ($E_{prim.nren}$), solar gains in July ($q_{sol.jul}$).

Parameter	Units	Limit	RF
$E_{prim.tot}$	kWh·m_n^2·$year^{-1}$	259.3	123.4
$E_{prim.nren}$	kWh·m_n^2·$year^{-1}$	113.8	120.1
$q_{sol.jul}$	kWh·m_n^2·$month^{-1}$	4	7.60

The results are further compared to cost-optimal study of Spanish building (Ministerio de Fomento, 2013), as shown in Table 13. This study only considers the heating and cooling demand, taking as reference a boiler efficiency of 0.75, a chiller performance of 1.7, natural gas primary energy factor of 1.07, and electricity primary energy factor of 2.464. Note the closest reference is for office buildings in B4 climate (the case of study corresponds to B3). This comparison, together with the results of the TOBEE project and the Spanish building code, confirm the representativity of the GESA building results, which is considered verified.

4.2. *Daylighting*

As presented in the previous section, the solar control and the transparent PV window solutions increase the lighting consumption due to their lower visible transparency, in comparison to the reference system. Fig. 10 details the impact of each type of window into the daylight autonomy and excessive illuminance in each lighting sector. The results show that the corner sectors of the building are very exposed to solar radiation, having good daylight autonomy but suffering of high amount of hours with illuminance above 2000 lux. The solar control and transparent PV windows significantly reduce the excessive illuminance time, although the daylight autonomy decreases in long stretches of the East and West zones. The inner zone has good daylight autonomy with the reference window, which greatly decreases with the new solution.

Table 13
Primary energy consumption of the case of study compared with Spanish cost-optimal report office building in B4 climate (Ministerio de Fomento, 2013).

	Units	Cost-optimal	RF
Primary energy consumption	kWh/m^2/year	89.6	89.2

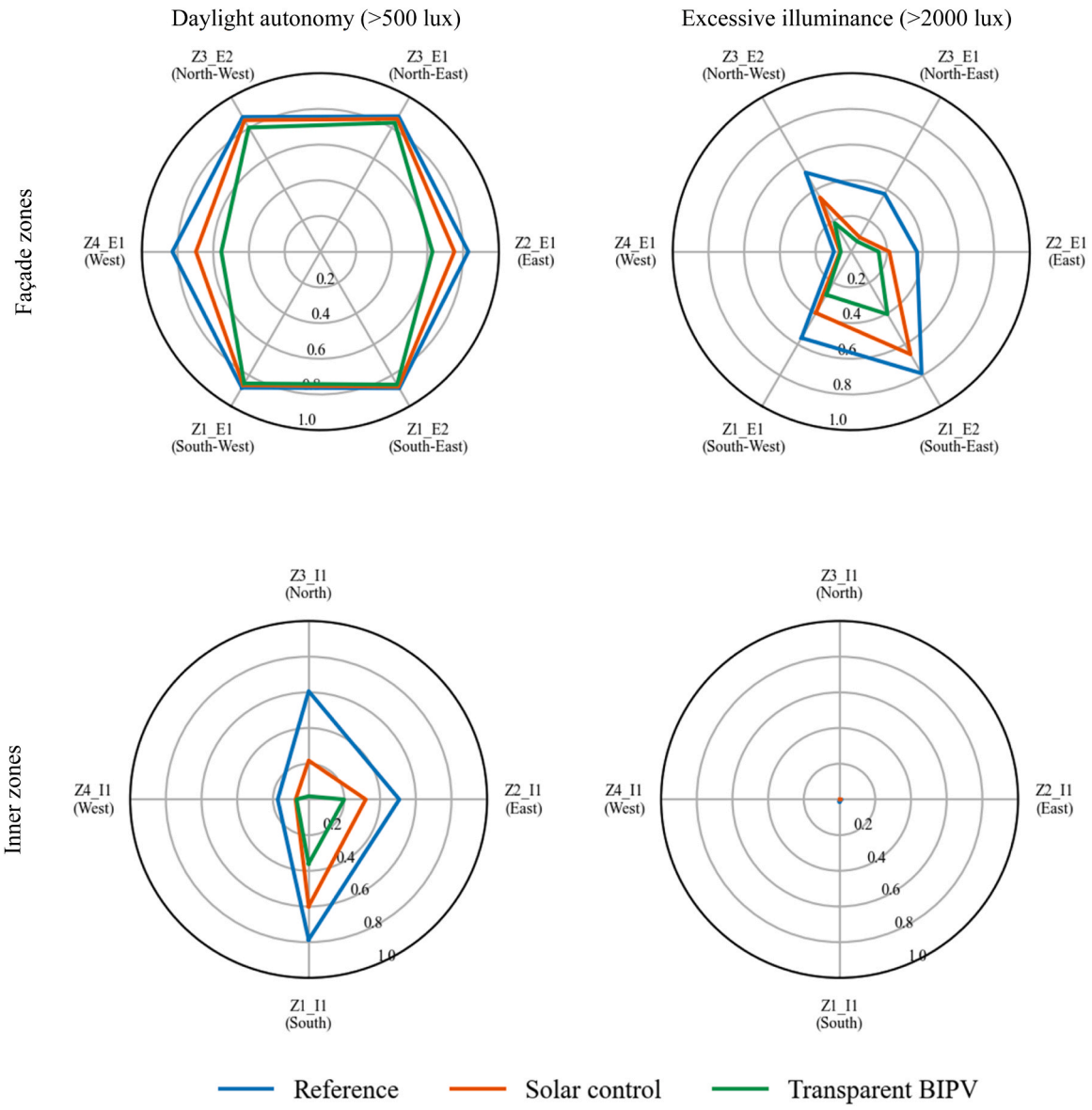

Fig. 10. Daylighting results.

The daylighting results points out that the building will probably require shading systems to ensure visual comfort of the occupant. This may reduce the daylight autonomy of some sectors, equalising the lighting consumption of the different window solutions.

4.3. Economic evaluation

The discounted payback of the four refurbishment solutions is summarised in Table 14. The solution with the best payback in all conditions is the SC window with opaque PV (SC+PV_{op}), while the transparent PV (PV_{tr}) alone has payback beyond 50 years. The electricity price profile highly influences in the payback of all solutions, with the California scenario making all scenarios, except SC+PV_{op} in 100% compensation, to have paybacks above 50 years. The building mainly consumes during the daylight hours due to the occupancy schedule and the cooling dominate loads. Hence, in the "high PV" scenario the main consumption and generation occurs in the "supervalley" period, meaning that the energy saving due to self-consumption have a reduced impact in the energy cost. Moreover, the feed-in tariff for excessive production PV is also very low. The compensation scenario has less influence in the payback, mainly due to 75% of the PV output being self-consumed, yet it may result in the payback decreasing by 2–6 years for the opaque SC+PV_{op} and PV_{tr}+PV_{op} solutions, respectively, in the current electricity price scenarios.

Table 14
Discounted payback period (in years).

Compensation	Price profile	SC	SC +PV_{op}	PV_{tr}	PV_{tr}+PV_{op}
0%	current	24	14	> 50	26
30%	current	24	14	> 50	24
100%	current	24	12	> 50	20
0%	high PV	> 50	> 50	> 50	> 50
30%	high PV	> 50	> 50	> 50	> 50
100%	high PV	> 50	40	> 50	> 50

The lower average electricity price and, more importantly, the timing of the generation in the "high PV" scenario explain the significantly worst payback periods. Fig. 11 details the electricity output in each price slot, according Fig. 4, of the transparent and opaque BIPV on each façade. As comparison, results of opaque PV panels in optimal orientation (south facing 39.1° slope) are also presented. In the "current" scenario, the PV output is relatively evenly distributed between

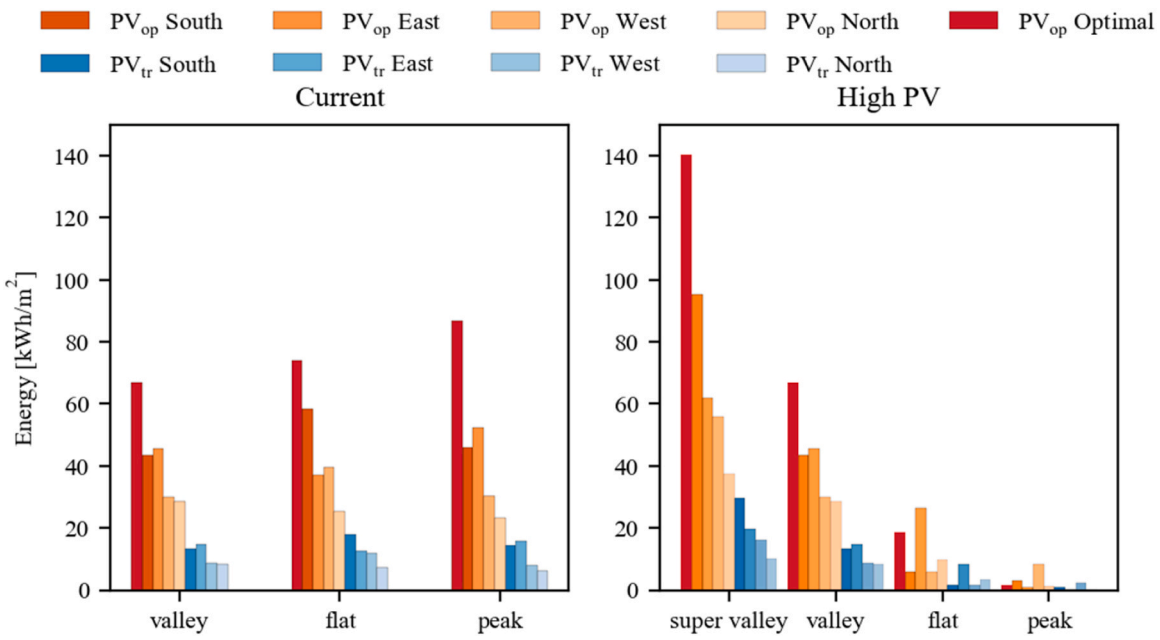

Fig. 11. PV output per price slot at current (left) and California (right) electricity price schedule scenarios.

electricity price slots (between 28% and 41% per slot). Noticeably, the optimal orientation has higher output in the more expensive slots. However, in the "high PV" scenario, almost all the generation occurs in the "super-valley" slot (as intended), decreasing significantly in the more expensive time slots (49–64% in "super-valley", 29–45% in "valley", and <20% in "flat" and "peak", depending on the orientation).

5. Discussion

The case of study consists of an old office building with highly inefficient envelope. This study only takes into account the refurbishment of the glazing system and integration of BIPV, both in the transparent and opaque sections of the envelope. The results show an improvement in the energy performance and visual comfort, but the economic evaluation presents some challenges for the solar control windows and transparent PV alone. Nevertheless, the building requires an integral intervention of the envelope in order to bring it to the current energy efficiency standards, also accounting the occupants thermal and visual comfort. In any case, the opaque PV showed great potential for improving the energy performance of the building.

In terms of energy demand, all the proposed solutions improve the overall energy performance of the existing system, especially on the cooling side. Yet, the lower visual transmittance of the solar control window and the transparent PV significantly increase the lighting demand (~22% and ~39% respectively). The difference in lighting demand may be overestimated because of the continuous daylighting control, which is implemented equally in all the simulation scenarios. This control could be considered as an improvement in the refurbished building, which would compensate the lower visible transparency of the refurbish solutions. Moreover, the study did not consider the use of shadings system to cope with the visual comfort requirements of occupants. As shown in the daylight results, the solar control window and the transparent PV reduce the hours of excessive daylight by ~25% and ~50%, which may be translated in a reduced need of shading systems and a better effective daylight autonomy.

Comparing the proposed solutions, the conventional solar control window presents better results than the transparent PV, with reduced heating, cooling, and lighting demand, as result of the better insulation, SHGC, and visual transparency. Nevertheless, the electric generation of the transparent PV improved the energy balance of the building (~11%). Moreover, the data for the transparent PV used in this study is based on a prototype currently in development, hence there is room to improve the thermal, optical, and electrical properties to better fit the building needs, as well as to increase the PV conversion efficiency.

In terms of energy balance, the BIPV solutions have a 31% of the generated electricity exported to the grid. This value is highly influenced by the operation regimes defined, which have nearly null energy consumption during non-occupancy hours. That means nearly all generation during the weekends is exported to the grid. A real building may have a base load consumption, which could partially use the PV generation even during non-occupancy hours. Moreover, the use of energy storage technologies or energy flexibility strategies may increase the self-consumption of PV output, decreasing the building energy demand to the grid and further improving its environmental impact.

The results of the opaque PV highlight the maturity and performance of this technology. Even with only 23% of the façade available and using non-optimal orientation the opaque PV significantly improve the building energy balance and have positive economic results, with the exception of the California scenario. In contrast, the prototype status of transparent PV solution implies some uncertainties on its final product properties, performance and cost. With the data used in the current article, the transparent PV has a good energy performance but presents poor payback results, with values above the life-span estimated for the panels. The case-study assumes that all the façades are refurbished with the same solution, despite the results show the West and North façades having 37% and 52%, respectively, less PV output than the best performing façade (South). Installation of transparent PV only in the better oriented façades will limit the total PV generation but may improve its economic feasibility. Nevertheless, the study assumes the refurbishment of the windows is mandatory. Considering this, the economic feasibility will depend on the balance between the BIPV window extra cost compared to the conventional window, the PV output, and the electricity cost. Moreover, the study assumed an investment cost of 228.29 €/m^2, which is a 60% higher than conventional opaque BIPV panels. The final cost is still uncertain and will depend on the final configuration, the technology maturity, and economies of scale. These issues are beyond the scope of the current article and will be tackled in further research.

Consequently, an analysis of the favourable scenarios for installing transparent PV is presented in Fig. 12, which presents a calculation of the maximum investment cost that achieves a discounted payback

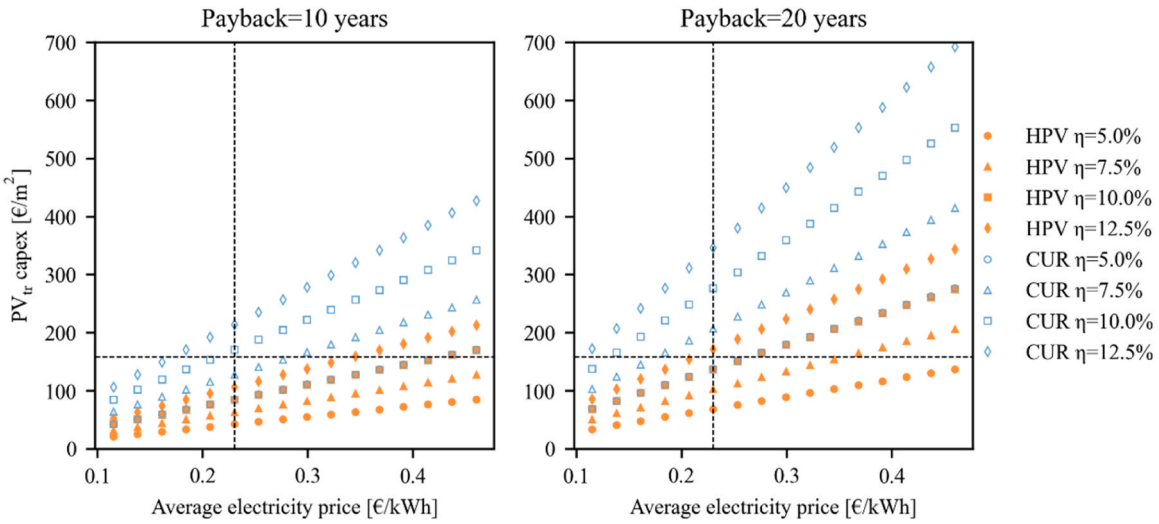

Fig. 12. East façade maximum PV_{tr} investment cost as function of the payback, average electricity price, pricing schedule, and efficiency. Horizontal dotted line is the PV_{op} investment cost. Vertical dotted line is the average electricity price used in this study. "CUR" and "HPV" refer to "current" and "high PV" price schedules, respectively.

period of 10 and 20 years as function of the average electricity price, the pricing schedule scenario, and the PV efficiency, assuming a compensation scenario of 30% of the electricity price. It is reasonable to assume that transparent PV will be more expensive than conventional PV (the reference cost is marked in the dotted horizontal line), due to its characteristics and the need to meet the glazing system requirements. Considering this and the current context of energy cost increase (the average electricity price used in this study is marked in the vertical dotted line), Fig. 12 shows the scenarios in which transparent PV will be feasible. These improve significantly if the efficiency can be improved above 5%.

The economic evaluation and the analysis in Fig. 12 showcase the relevance of the electricity pricing schemes into the promotion of BIPV. The duck chart of the California scenario has the goal to incentive consumption during high PV generation periods. However, it may discourage the deployment of BIPV from the pure economical point of view. BIPV reduce the building energy balance, hence the demand to the grid, and reduce the need to further occupy land for energy generation, reducing social discontent, NIMBY phenomenon, and land uses conflicts. These factors need to be considered in policies to promote deployment of BIPV. On top of that, the case study presented is representative of a typology of existing buildings. Compared to the current standards, these buildings are energy inefficient and require an integral refurbishment of the envelope and energy systems. A holistic intervention of the building may open more opportunities for implementing the BIPV, both in the opaque and transparent of the envelope, in an efficient way.

6. Conclusions

The article presents a simulation study of the impact of building integrated photovoltaics (BIPV) on isolated high rise highly glazed office buildings. The study takes as reference a representative floor of the GESA building in Palma de Mallorca (Spain). The study considers the refurbishment of the glazing system and the integration of BIPV on the opaque and transparent sections, without changing the façade design due its protection by the local heritage commission. A comprehensive building model integrating the BIPV impact in walls in windows for the thermal, electrical and daylighting simulation based on a modification of TRNSYS18 complex fenestration model is considered. The solutions for the glazing system include a conventional solar control window and a transparent photovoltaic prototype window. On the opaque part, conventional BIPV is considered.

The results show the potential of the BIPV solutions for improving the energy balance of the building. The transparent PV reduced the energy demand by 6.9% and the total energy balance by 21%. The opaque PV further improved the results of the two glazing system solutions, the energy balance improving to 28.1% and 38.3% with the solar control and transparent PV solutions, respectively.

On the daylighting side, the proposed transparent PV glazing system solutions have worst daylighting autonomy, leading to a higher lighting demand. This is related to the lower transparency associated to a better solar heat gain coefficient (SHGC) and absorption of the transparent PV. Yet, these characteristics also helped to reduce the hours with excessive daylighting (>2000 lux), which is a relevant problematic in highly glazed and exposed buildings. As a result, solutions like transparent PV windows may help to improve the visual comfort and reduce the need of shading systems.

The economic evaluation highlights the relevance of electricity pricing policies into the promotion of BIPV. Duck chart schemes reduce the economic savings of BIPV by lowering electricity prices during high solar generation periods. However, BIPV help to reduce the building electricity demand from the grid, improving its autonomy and reducing its environmental impact.

Finally, the study considered a transparent PV prototype window. The technology used is still in development, with some uncertainties on the final optical, thermal, electrical, and economic characteristics. Yet, the results show the capabilities of this technology and provides guidelines for investment cost and efficiency targets. Further studies should analyse the balance between optical properties (daylighting, visual comfort, and aesthetics), thermal performance, and efficiency.

CRediT authorship contribution statement

Alba Ramos: Conceptualization, Formal analysis, Investigation, Methodology, Software, Validation, Writing – original draft, Writing – review & editing. **Joaquim Romaní**: Conceptualization, Formal

analysis, Methodology, Software, Visualization, Writing – original draft, Writing – review & editing. **Jaume Salom**: Formal analysis, Project administration, Resources, Supervision, Writing – review & editing.

Declaration of Competing Interest

The authors declare that they have no known competing financial interests or personal relationships that could have appeared to influence the work reported in this paper.

Data availability

Data will be made available on request.

Acknowledgements

This work has received funding from the European Union H2020 Framework Programme under Grant Agreement number 826002 (Tech4Win). This project has received funding from the European Union's H2020 research and innovation programme under grant agreement number 101036723 (ARV – Climate Positive Circular Communities). Alba Ramos acknowledges the Universitat Politècnica de Catalunya for her Serra Hunter professor post. Joaquim Romaní would like to thank Ministerio de Economía y Competitividad de España for Grant Juan de la Cierva FJC2018-038475-I. All researchers from IREC have been partially supported by Departament de Recerca i Universitats, Generalitat de Catalunya 2021 SGR 01403.

References

Alrashidi, H., Issa, W., Sellami, N., Sundaram, S., Mallick, T., 2022. Thermal performance evaluation and energy saving potential of semi-transparent CdTe in Façade BIPV. Sol. Energy 232, 84–91. https://doi.org/10.1016/j.solener.2021.12.037.

Athens Towers, 2022. ⟨https://en.wikipedia.org/wiki/Athens_Towers⟩ (Last accessed 1st July 2022).

Attoye, D.E., Aoul, K.A.T., Hassan, A., 2017. A review on building integrated photovoltaic façade customization potentials. Sustainability 9 (12), 2287. https://doi.org/10.3390/su9122287.

Azami, A., Sevinç, H., 2021. The energy performance of building integrated photovoltaics (BIPV) by determination of optimal building envelope. Build. Environ. 199, 107856 https://doi.org/10.1016/j.buildenv.2021.107856.

Bambara, J., Athienitis, A.K., 2019. Energy and economic analysis for the design of greenhouses with semi-transparent photovoltaic cladding. Renew. Energy 131, 1274–1287. https://doi.org/10.1016/j.renene.2018.08.020.

BEDEC, 2022. Proyecto y obra. Banco Construcción 2021–01. ⟨https://metabase.itec.es/vide/es/bedec⟩ (accessed Jan. 10, 2022).

Bellazzi, A., Belussi, L., Meroni, I., 2018. Estimation of the performance of a BIPV façade in working conditions through real monitoring and simulation. Energy Procedia 148, 479–486. https://doi.org/10.1016/j.egypro.2018.08.123.

Biyik, E., et al., 2017. A key review of building integrated photovoltaic (BIPV) systems. Eng. Sci. Technol. Int. J. 20 (3), 833–858. https://doi.org/10.1016/j.jestch.2017.01.009.

Chen, L., Zheng, X., Yang, J., Yoon, J.H., 2021. Impact of BIPV windows on building energy consumption in street canyons: model development and validation. Energy Build. 249, 111207 https://doi.org/10.1016/j.enebuild.2021.111207.

Código técnico de la edificación, 2019. Documento básico HE, Ahorro de energía. Ministerio de transportes, movilidad y agenda urbana. Ministerio de transportes, movilidad y agenda urbana.

Denholm, P., O'Connell, M., Brinkman, G., Jorgenson, J., 2015. Overgeneration from Solar Energy in California: A Field Guide to the Duck Chart. NREL.

Edifici Seat, 2022. ⟨https://www.poblesdecatalunya.cat/element.php?e=10314⟩ (Last accessed 1st July 2022).

European Committee for Standardization, 2011. EN 12464–1:2011 Light and lighting – Lighting of work places. Part 1: Indoor work places. European Committee for Standardization, Brussels, Belgium.

Eurostat, 2021. Electricity Price Statistics. ⟨https://ec.europa.eu/eurostat/statistics-explained/index.php?title=Electricity_price_statistics⟩ (Accessed Dec. 23, 2021).

Eurostat, 2022. HCIP Annual Data (Average Index and Rate of Change). ⟨https://ec.europa.eu/eurostat/databrowser/view/PRC_HICP_AIND/default/table?lang=en⟩ (Accessed Jan. 24, 2022).

Fraunhofer, I.S.E., 2020. Photovoltaics Report, Freiburg (Germany).

Freitas, J. de S., Cronemberger, J., Soares, R.M., Amorim, C.N.D., 2020. Modeling and assessing BIPV envelopes using parametric Rhinoceros plugins Grasshopper and Ladybug. Renew. Energy 160, 1468–1479. https://doi.org/10.1016/j.renene.2020.05.137.

Goncalves, J.E., van Hooff, T., Saelens, D., 2020. A physics-based high-resolution BIPV model for building performance simulations. Sol. Energy 204, 585–599. https://doi.org/10.1016/j.solener.2020.04.057.

Hiller, M., Schöttl, P., 2014. Modellierung komplexer verglasungssysteme in TRNSYS. BauSim2014, pp. 387–394.

IDAE, 2016. Factores de emisión de CO2 y coeficientes de paso a energía primari de diferentes fuentes de energía final consumidas en el sectors de edificios de España. Ministerios de Industria, Energía y Turismo y Ministerio de Fomento de España.

IDAE, 2012. Guía técnica: Instalacions de climatización con equipos autónomos. Ministerio de industria, energía y turismo de España. ⟨https://www.idae.es/uploads/documentos/documentos_17_Guia_tecnica_instalaciones_de_climatizacion_con_equipos_autonomos_5bd3407b.pdf⟩.

IEA, 2019. Global Status Report for Buildings and Construction 2019 – Analysis, Paris (France).

IEA, 2020. Tracking Buildings 2020 – Analysis, Paris (France).

International Energy Agency, 2021. Spain 2021, Energy Policy Review. International Energy Agency (IEA). ⟨https://www.iea.org/reports/spain-2021⟩ (last accessed Jun. 21, 2022).

IPCC, 2018. Global Warming of 1.5 ºC.

IRENA, 2020. Renewable Power Generation Costs in 2019. Abu Dhabi (United Arab Emirates).

ISO 15099, 2003. Thermal Performance of Windows, Doors and Shading Devices – Detailed Calculations. International Organization for Standardization.

Jelle, B.P., Breivik, C., Drolsum Røkenes, H., 2012. Building integrated photovoltaic products: a state-of-the-art review and future research opportunities. Sol. Energy Mater. Sol. Cells 100, 69–96. https://doi.org/10.1016/j.solmat.2011.12.016.

Kumar, A., Bieri, M., Reindl, T., Aberle, A.G., 2017. Economic viability analysis of silicon solar cell manufacturing: Al-BSF versus PERC. Energy Procedia 130, 43–49. https://doi.org/10.1016/j.egypro.2017.09.412.

Lawrence Berkeley National Laboratory, 2013. OPTICS. ⟨https://windows.lbl.gov/software/optics⟩ (Accessed Jan. 07, 2022).

Lawrence Berkeley National Laboratory, 2021. International Glazing Data Base (IGDB), 2021. ⟨https://windows.lbl.gov/software/igdb⟩ (Accessed Jan. 07, 2022).

Lawrence Berkeley National Laboratory, 2022. WINDOW7. ⟨https://windows.lbl.gov/software/window⟩ (Accessed Jan. 07, 2022).

Magrini, A., Lentini, G., Cuman, S., Bodrato, A., Marenco, L., 2020. From nearly zero energy buildings (NZEB) to positive energy buildings (PEB): the next challenge - the most recent European trends with some notes on the energy analysis of a forerunner PEB example. Dev. Built Environ. 3, 100019 https://doi.org/10.1016/J.DIBE.2020.100019.

Meng, W., Jinqing, P., Hongxing, Y., Yimo, L., 2018. Performance evaluation of semi-transparent CdTe thin film PV window applying on commercial buildings in Hong Kong. Energy Procedia 152, 1091–1096. https://doi.org/10.1016/j.egypro.2018.09.131.

Meraj, M., Khan, M.E., 2019. Thermal modeling of opaque and semi-transparent photovoltaic (PV) module. Int. J. Innov. Technol. Explor. Eng. 8 (12), 3271–3276. https://doi.org/10.35940/ijitee.L3616.1081219.

Ministerio de Fomento, 2013. Report on Cost Optimal Calculations and Comparison with the Current and Future Energy Performance Requirements of Buildings in Spain. Ministerio de Fomento de España.

Nabil, A., Mardaljevic, J., 2005. Useful daylight illuminance: a new paradigm to access daylight in buildings. Light. Res. Technol. 37 (1), 41–59. https://doi.org/10.1191/1365782805li128oa.

Olivieri, L., Caamaño-Martín, E., Moralejo-Vázquez, F.J., Martín-Chivelet, N., Olivieri, F., Neila-Gonzalez, F.J., 2014. Energy saving potential of semi-transparent photovoltaic elements for building integration. Energy 76, 572–583. https://doi.org/10.1016/j.energy.2014.08.054.

Paricio, I., 2015. Informe sobre la fachada del edificio antigua sede de GESA, Barcelona (Spain).

Pascual, J., 2015. Directrices energéticas integrals en edificios de oficinas transparentes (TOBEE). Radiografia del edificio de oficinas para un clima Mediterráneo (Ph.D. thesis). Universitat Politécnica de Catalunya.

Pascual, J., Casanova, M., Tavan, D., 2010. Multidimensional performance analysis of office buildings with highly glazed facades. How do they perform in a Mediterranean climate? In: Proceedings of the 3rd International Conference Palenc 2010, Passive and Low Energy Cooling for the Built Environment, Rhodes Island, Greece.

Pranith, S., Bhatti, T.S., 2015. Modeling and parameter extraction methods of PV modules-review. In: Proceedings of the International Conference on Recent Developments in Control, Automation and Power Engineering, RDCAPE 2015, pp. 72–76. DOI: ⟨10.1109/RDCAPE.2015.7281372⟩.

Quesada, G., Rousse, D., Dutil, Y., Badache, M., Hallé, S., 2012. A comprehensive review of solar facades. Transparent and translucent solar facades. Renew. Sustain. Energy Rev. 16 (5), 2643–2651. https://doi.org/10.1016/j.rser.2012.02.059.

Ramanujam, J., et al., 2020. Flexible CIGS, CdTe and a-Si:H based thin film solar cells: a review. Prog. Mater. Sci. 110, 100619 https://doi.org/10.1016/j.pmatsci.2019.100619.

Reinhart, C.F., Mardaljevic, J., Rogers, Z., 2006. Dynamic daylight performance metrics for sustainable building design. LEUKOS J. Illum. Eng. Soc. N. Am. 3 (1), 7–31. https://doi.org/10.1582/LEUKOS.2006.03.01.001.

Roeleveld, D., Hailu, G., Fung, A.S., Naylor, D., Yang, T., Athienitis, A.K., 2015. Validation of computational fluid dynamics (CFD) model of a building integrated photovoltaic/thermal (BIPV/T) system. Energy Procedia 78, 1901–1906. https://doi.org/10.1016/j.egypro.2015.11.359.

Romaní, J., Hiller, M., Salom, J., 2021a. Modelling of transparent PV windows with complex fenestration systems in TRNSYS. In: Proceedings of the 17th IBPSA

Conference, Bruges (Belgium), pp. 1649–1656. DOI: ⟨10.26868/25222708.2021.30486⟩.
Romaní, J., Szambolics, H., Jimenez, M., Calvo, S., Pérez-Rodríguez, A., Salom, J., 2021b. Evaluation of the implementation of a BIPV glass in office buildings in Spain. In: Proceedings of the ISES Solar World Congress, SWC2021, pp. 152–163. DOI: ⟨10.18086/swc.2021.09.02⟩.
Saadon, S., Gaillard, L., Giroux-Julien, S., Ménézo, C., . 2016. Simulation study of a naturally-ventilated building integrated photovoltaic/thermal (BIPV/T) envelope. Renew. Energy vol. 87, 517–531. https://doi.org/10.1016/J.RENENE.2015.10.016.
Sánchez-Palencia, P., Martín-Chivelet, N., Chenlo, F., 2019. Modeling temperature and thermal transmittance of building integrated photovoltaic modules. Sol. Energy 184, 153–161. https://doi.org/10.1016/j.solener.2019.03.096.
Seagram Building, 2022. ⟨https://en.wikipedia.org/wiki/Seagram_Building⟩ (Last accessed 1st July 2022).
Solar Module, 2022. Standard-PV-Module – L of Solar – Color Solar Cell. ⟨http://www.lofsolar.com/Standard-PV-Module#6⟩ (Accessed Jan. 09, 2022).
Sun, H., Heng, C.K., Tay, S.E.R., Chen, T., Reindl, T., 2021. Comprehensive feasibility assessment of building integrated photovoltaics (BIPV) on building surfaces in high-density urban environments. Sol. Energy 225, 734–746. https://doi.org/10.1016/j.solener.2021.07.060.
SYNIKIA, 2021. D. 2.1 Report on Design plus Energy Neighbourhoods in Each of the Four Climatic Types.
Tech4win, 2019. Disruptive Sustainable Technologies for next Generation PV Windows. ⟨http://www.tech4win.eu/⟩ (Accessed Jan. 09, 2022).
TESS, 2013. TESSLibs17 Component Libraries for the TRNSYS Simulation Environment. Volume 03 – Electrical Library Mathematical Reference. Thermal Energy Systems Specialists. Madison, Wisconsin (USA).
TESS, 2017. TRNSYS 18. ⟨https://www.trnsys.com/⟩ (Last accessed 20/04/2022).
The European Commission, 2010. Directive 2010/31/EU on the Energy Performance of Buildings, Brussels (Belgium).
The European Commission, 2012. Directive 2012/27/EU on Energy Efficiency.
The European Commission, 2018. Directive (EU) 2018/844 of the European Parliament and of the Council of 30 May 2018 Amending Directive 2010/31/EU on the Energy Performance of Buildings and Directive 2012/27/EU on Energy Efficiency (Text with EEA Relevance).
The European Commission, 2019. The European Green Deal Brussels (Belgium).
TRANSSOLAR, 2018. TRNSYS 18 - A Transient System Simulation Program: Multizone Building Modelling with Type56, Volume 5. University of Wisconsin-Madison, Madison, WI, USA.
Virtuani, A., Strepparava, D., 2017. Modelling the performance of amorphous and crystalline silicon in different typologies of building-integrated photovoltaic (BIPV) conditions. Sol. Energy 146, 113–118. https://doi.org/10.1016/j.solener.2017.02.035.
Xiong, W., Liu, Z., Wu, Z., Wu, J., Su, F., Zhang, L., 2022. Investigation of the effect of inter-building effect on the performance of semi-transparent PV glazing system. Energy 245, 123160. https://doi.org/10.1016/j.energy.2022.123160.
Yang, S., Cannavale, A., Di Carlo, A., Prasad, D., Sproul, A., Fiorito, F., 2020. Performance assessment of BIPV/T double-skin façade for various climate zones in Australia: effects on energy consumption. Sol. Energy 199, 377–399. https://doi.org/10.1016/j.solener.2020.02.044.